

Fig. 3 Response with adaptive output feedback controller: a) spacecraft attitude θ and b) fuel slosh angle λ .

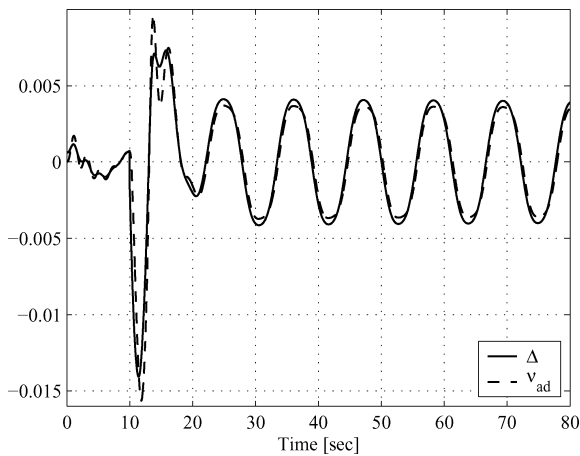


Fig. 4 Computed model inversion error Δ and its NN estimate ν_{ad} .

slowly decaying fuel sloshing. This slow decay is attributed to the fact that the only mechanism for absorbing the fuel motion, while the spacecraft attitude is almost constant, is the small friction force. The adaptive controller eliminates the excitation of the sloshing mode and dramatically reduces its effect on the attitude response. This is illustrated in the insert at the top of Fig. 3, which shows a small decaying oscillation with an amplitude of about 0.075 deg at 80 s. The performance of the adaptive element is shown in Fig. 4, which shows a close match between the computed model inversion error Δ and the adaptive signal ν_{ad} .

Conclusions

This Note presents a nonstandard feedback linearization scheme that can enhance model-inversion-based control design paradigms. This scheme is examined in conjunction with a recently published direct output feedback design approach for nonlinear SISO systems with known relative degree. The controller synthesis comprises the proposed feedback linearization scheme coupled with a linear compensator design and an adaptive NN-based element used to reduce the effect of model inversion errors. Prior knowledge or partial information about the open-loop system dynamics can be incorporated in the design through the proposed linearization procedure. Consequently, the design of the linear compensator can be simplified, usually leading to lower-order compensators. This feature is particularly important for systems with relative degree greater than two, where the linear design step can be challenging. The stability proof provides important design and parameter tuning guidelines, which are instrumental in ensuring uniform ultimate boundedness of the closed-loop system errors.

Acknowledgments

This research was partly sponsored by the fund for the promotion of research at the Technion and by U.S. Air Force Office of Scientific Research Contracts F49620-01-1-0024 and F49620-03-1-0443.

References

- ¹Chen, F. C., and Khalil, H. K., "Adaptive Control of Nonlinear Systems using Neural Networks," *International Journal of Control*, Vol. 55, No. 6, 1992, pp. 1299–1317.
- ²Kim, Y., and Lewis, F. L., *High Level Feedback Control with Neural Networks*, World Scientific, River Edge, NJ, 1998.
- ³Rysdyk, R., and Calise, A. J., "Nonlinear Adaptive Flight Control Using Neural Networks," *IEEE Controls Systems Magazine*, Vol. 18, No. 6, 1998, pp. 14–25.
- ⁴Calise, A. J., Hovakimyan, N., and Idan, M., "Adaptive Output Feedback Control of Nonlinear Systems Using Neural Networks," *Automatica*, Vol. 37, No. 8, 2001, pp. 1201–1211.
- ⁵Hovakimyan, N., Nardi, F., Calise, A. J., and Kim, N., "Adaptive Output Feedback Control of Uncertain Systems Using Single Hidden Layer Neural Networks," *IEEE Transactions on Neural Networks*, Vol. 13, No. 6, 2002, pp. 1420–1431.
- ⁶Isidori, A., *Nonlinear Control Systems*, Springer-Verlag, Berlin, 1995.
- ⁷Brasch, J., and Pearson, J., "Pole Placement using Dynamic Compensators," *IEEE Transactions on Automatic Control*, Vol. 15, No. 1, 1970, pp. 34–43.
- ⁸Lavretsky, E., Hovakimyan, N., and Calise, A. J., "Upper Bounds for Approximation of Continuous-Time Dynamics Using Delayed Outputs and Feedforward Neural Networks," *IEEE Transactions on Automatic Control*, Vol. 48, No. 9, 2003, pp. 1606–1610.
- ⁹Bryson, A. E. J., *Control of Spacecraft and Aircraft*, Princeton Univ. Press, Princeton, NJ, 1994, pp. 129–131.

Guidance of Unmanned Air Vehicles Based on Fuzzy Sets and Fixed Waypoints

Mario Innocenti,* Lorenzo Pollini,[†]
and Demetrio Turra[‡]

University of Pisa, 56126 Pisa, Italy

I. Introduction

THE problem of guidance and control of unmanned aerial vehicles (UAVs) has become a topic of research in recent years. Typical projected UAV operations such as surveillance, payload delivery, and search and rescue can be addressed by waypoint-based guidance. Automatic target recognition, for instance, requires that the aircraft approach the possible target from one or more desired directions. In a highly dynamic cooperative UAV environment, the management system, either centralized or decentralized, may switch the waypoint set rapidly to change an aircraft mission depending on external events, pop-up threats, etc.; the new waypoint set may be ill-formed in terms of flyability (maximum turn rates, descent speed, acceleration, etc.). Although fuzzy logic methods have been applied in the past—see for instance Ref. 1, where Mamdani rules were

Presented as Paper 2002-4993 at the Guidance, Navigation and Control, Monterey, CA, 8 August 2002; received 26 May 2003; revision received 30 October 2003; accepted for publication 11 November 2003. Copyright © 2003 by the American Institute of Aeronautics and Astronautics, Inc. All rights reserved. Copies of this paper may be made for personal or internal use, on condition that the copier pay the \$10.00 per-copy fee to the Copyright Clearance Center, Inc., 222 Rosewood Drive, Danvers, MA 01923; include the code 0731-5090/04 \$10.00 in correspondence with the CCC.

*Full Professor, Department of Electrical Systems and Automation. Associate Fellow AIAA.

[†]Postdoctoral Fellow, Department of Electrical Systems and Automation.

[‡]Ph.D. Student, Department of Electrical Systems and Automation.

used—traditional proportional navigation² techniques preclude the specification of a desired waypoint's crossing direction, possibly producing flight paths that are not feasible for a generic UAV. The present Note describes an alternate guidance scheme for path planning and trajectory computation by specifying the waypoint position in space, crossing heading, and velocity. The procedure is based on a fuzzy controller that commands the aircraft, via its autopilot, to approach a specified set of waypoints. The use of a fuzzy approach, as supposed to other methods, is justified by the current interest in generating additional intelligence onboard autonomous vehicles. Since the implementation of fuzzy guidance systems (FGS) may become very expensive in terms of computational load, the present approach is based on Takagi–Sugeno fuzzy sets,³ known for their limited computational requirements. As standard practice in most guidance studies,⁴ a simple first-order dynamic model for the autopiloted aircraft dynamics is used in the controller design phase. Simulation results, which show the behavior of the proposed guidance structure using the simple first-order model and a fully nonlinear aircraft model with LQG–LTR-based autopilots, are included.

II. Aircraft Modeling and Control

The aircraft guidance problem is addressed by assuming the presence of an inner autopilot loop for tracking commanded velocity, flight path, and heading, as well as providing adequate disturbance rejection and robustness. The outer-loop FGS generates a reference for the autopilots in order to reach the desired waypoint. It is assumed that the aircraft plus autopilot model can track desired velocity, flight path angle, and heading angle with first-order dynamic behavior, given as follows:

$$\dot{V} = k_v(V_d - V), \quad \dot{\gamma} = k_\gamma(\gamma_d - \gamma), \quad \dot{\chi} = k_\chi(\chi_d - \chi) \quad (1)$$

where the state vector is given by velocity V and flight path γ , and heading χ angles, $\bar{x} = [V \ \gamma \ \chi]^T$, and the inputs are the desired state $[V_d \ \gamma_d \ \chi_d]^T$, with the gains k_i being positive constants.^{5,6} Metric units are used, with angles expressed in degrees.

III. Fuzzy Guidance

The overall guidance scheme has two components: a waypoint generator (WG) and the actual fuzzy guidance system. The desired trajectory is specified in terms of a sequence of waypoints without any requirement on the path between two successive waypoints. A waypoint is described using a standard right-handed Cartesian reference frame (X_w, Y_w, H_w) , and the desired crossing speed and heading angle (V_w, χ_w) are used to obtain a preferred approaching direction and velocity; thus the waypoint belongs to a five-dimensional space W . The WG holds a list of waypoints in five dimensions, checks aircraft position, and updates the desired waypoint when the previous one has been reached within a given tolerance. The waypoint generator's only task is to present the actual waypoint to the FGS. Since the main purpose of the work was the validation of a fuzzy-set guidance law, no dead-reckoning or navigational errors were included; rather a tolerance “ball” was included around the waypoint, defining that as actual target reached.

Between the WG and the FGS, a coordinate transformation (single rotation) is performed to convert Earth-fixed-frame position errors into waypoint-frame components. Each waypoint defines a coordinate frame centered at the waypoint position (X_w, Y_w, H_w) and rotated by (χ_w) around the H -axis. The coordinate transformation allows the synthesis of a fuzzy rule-set valid in the waypoint-fixed coordinated frame, which is invariant with respect to the desired approach direction (χ_w) . When a waypoint is reached, the next one is selected, the actual reference value W is changed, and the rotation matrix is updated to transform position and orientation errors into the new waypoint coordinate frame.

As described earlier, the aircraft autopilots were designed to track desired airspeed and heading and flight path angles $[V_d \ \gamma_d \ \chi_d]^T$, using decoupled closed loop inner dynamics, and so three independent Takagi–Sugeno fuzzy controllers were synthesized to constitute the FGS. The first generates the desired flight path angle γ_d for the

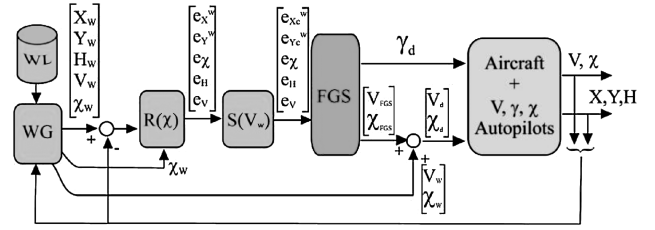


Fig. 1 Complete fuzzy guidance and control diagram.

autopilot using altitude error $e_H = H_w - H$ as

$$\gamma_d = f_\gamma(e_H) \quad (2)$$

The second computes desired aircraft velocity:

$$V_d = V_w + f_V(V - V_w) = V_w + f_V(e_V) \quad (3)$$

The third is responsible for the generation of the desired heading angle (χ_d) using the position errors along the X and Y axes in the current waypoint-frame $(e_{X_c}^w, e_{Y_c}^w)$ and the heading error e_χ . A fuzzy rule-set designed at a specified trim airspeed value could yield insufficient tracking performance when the desired waypoint crossing-speed (V_w) differed significantly from V . To accommodate large values of $(V - V_w)$ and to investigate at a preliminary level the effect of disturbances, modeled as vehicle's speed differential with respect to waypoint crossing-speed (V_w) , a speed-correlated scale coefficient of position error was introduced. Let us define

$$\text{Rot}(\chi_w) = \begin{bmatrix} \cos\left(\chi_w + \frac{\pi}{2}\right) & \sin\left(\chi_w + \frac{\pi}{2}\right) \\ -\sin\left(\chi_w + \frac{\pi}{2}\right) & \cos\left(\chi_w + \frac{\pi}{2}\right) \end{bmatrix} \quad (4)$$

The position errors in the fixed waypoint coordinates frame are given by

$$\begin{bmatrix} e_X^w \\ e_Y^w \end{bmatrix} = \text{Rot}(\chi_w) \cdot \begin{bmatrix} E_X^w \\ E_Y^w \end{bmatrix} = \text{Rot}(\chi_w) \cdot \begin{bmatrix} X - X_w \\ Y - Y_w \end{bmatrix} \quad (5)$$

The velocity-compensated position errors $(e_{X_c}^w, e_{Y_c}^w)$ are defined by

$$\begin{bmatrix} e_{X_c}^w \\ e_{Y_c}^w \end{bmatrix} = S(V^w, V^*) \begin{bmatrix} e_X^w \\ e_Y^w \end{bmatrix}, \quad \text{with} \quad S(V^w, V^*) = \frac{V^*}{V^w} \quad (6)$$

where V^* represents the airspeed value used during FGS membership rules design. In this way, position errors, used by the FGS to guide the aircraft toward the waypoint with desired approach direction, are magnified when V^w (requested waypoint crossing-speed) is larger than V^* or reduced otherwise. Equation (6) may diverge if V^w goes to zero; however, this is not an operationally relevant condition because the requested waypoint crossing-speed should be defined according to aircraft flight parameters. The definition of the parameter S denotes a new degree of freedom in the FGS tuning process and may also be defined using a nonlinear function of (V^w, V^*) provided that $S = 1$ when $V^w = V^*$. Finally, the desired heading angle produced by fuzzy controller is

$$\chi_d = \chi_w + f_\chi(e_{X_c}^w, e_{Y_c}^w, e_\chi) \quad (7)$$

The schematic of the overall system is shown in Fig. 1.

IV. Fuzzy Guidance Design

The fuzzy guidance system is based on a Takagi–Sugeno fuzzy systems (see Refs. 3 and 5) model described by a blending of fuzzy if–then rules. Using a weighted average defuzzifier layer each fuzzy controller output is defined as follows:

$$y = \frac{\sum_{k=1}^m \mu_k(x) u_k}{\sum_{k=1}^m \mu_k(x)} \quad (8)$$

where $\mu_i(x) u_i$ is the i th membership function of input x to i th fuzzy zone. The membership functions are a combination of Gaussian

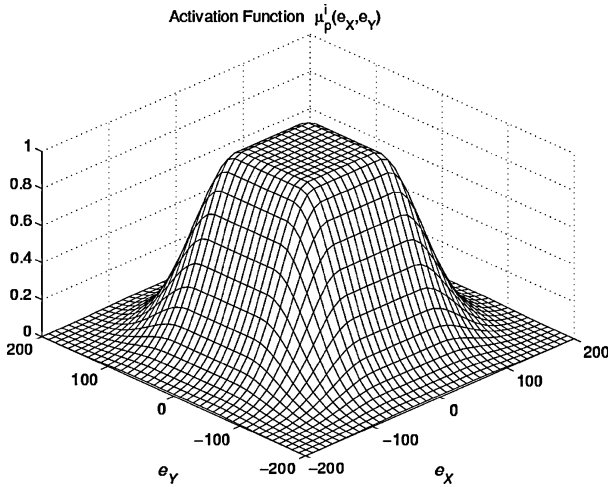


Fig. 2 General form for the membership functions on the error plane XY .

curves of the form

$$f(x, \sigma, c) = e^{-(x-c)^2/\sigma^2}$$

The general shape in the activation areas is shown in Fig. 2. Reference 6 contains the complete listing of all of the fuzzy rules used to create the fuzzy controllers.

The fuzzy rules were defined according to the desired approach direction and the angular rate limitations of the aircraft. The fuzzy knowledge base was designed to generate flyable trajectories using the maximum linear and angular velocities and accelerations that are typical of a small propeller-engine aircraft.^{7–9}

The FGS provides different desired flight path and heading angle commands for different values of distance from the waypoint. The altitude and velocity controllers are implemented using a Takagi–Sugeno model directly. For the altitude, the input is the altitude error $e_H = H - H_w$ and the output is the desired flight path angle γ_d . Input and output are mapped with four fuzzy sets each:

- If e_H is N_∞ then γ_d is P_{20} : for big negative errors.
- If e_H is N_s then γ_d is P_2 : for small negative errors.
- If e_H is P_s then γ_d is N_2 : for small positive errors.
- If e_H is P_∞ then γ_d is N_{20} : for big positive errors.

Here the generic output constant P_X represents the output value X and the constant N_X represents the output value $-X$.

The velocity controller is similar to the altitude controller. Three input fuzzy sets are used for the velocity error e_V and three for the resulting ΔV_d output:

- If e_V is N_∞ then ΔV_d is P_{10} : for negative errors.
- If e_V is ZE then ΔV_d is P_0 : for near to zero errors.
- If e_V is P_∞ then ΔV_d is N_{10} : for positive errors.

Here the generic output constant P_X represents the output value X and the constant N_X represents the output value $-X$.

Guidance in the horizontal (X – Y) plane is more complex. The horizontal plane fuzzy controller takes its input from scaled position errors ($e_{X_c}^w, e_{Y_c}^w$) and heading error e_χ . The error along the X axis is coded into five fuzzy sets:

- N_∞ : for big negative lateral errors.
- N_s : for small negative lateral errors.
- ZE : for near exact alignment.
- P_s : for small positive lateral errors.
- P_∞ : for big positive lateral errors.

Three sets (N_s, ZE, P_s) are also defined for the Y^w axis error ($e_{Y_c}^w$): ZE = aircraft over the waypoint, N_s = waypoint behind the aircraft, and P_s = waypoint in front of the aircraft. Finally, the heading error is coded into seven fuzzy sets. In the application of Eq. (8), the m fuzzy rules are grouped into S groups, each with K rules: $m = SK$. In the present work we used $S = 15$ and $K = 7$. The S groups cor-

respond to S areas on the XY plane. From the preceding,

$$\begin{aligned} y &= \frac{1}{c(x)} \sum_{i=1}^S \sum_{j=1}^K \mu_i^{xy}(e_{X_c}^w, e_{Y_c}^w) \cdot \mu_{ij}^x(e_\chi) u_{ij} \\ &= \frac{1}{c(x)} \sum_{i=1}^S \mu_i^{xy}(e_{X_c}^w, e_{Y_c}^w) \cdot \delta_{ij}^x(e_\chi) u_{ij} \end{aligned} \quad (9)$$

where

$$\begin{aligned} c(x) &= \sum_{k=1}^S \mu_k(x), & \delta_{ij}^x &= \sum_{j=1}^K \mu_{ij}^x(e_\chi) u_{ij} \\ \mu_i^{xy}(e_{X_c}^w, e_{Y_c}^w) &= \mu_i^x(e_{X_c}^w) \cdot \mu_i^y(e_{Y_c}^w) \end{aligned} \quad (10)$$

Equation (9) can be simplified as

$$y = \sum_{i=1}^S \frac{\mu_i^{xy}(e_{X_c}^w, e_{Y_c}^w)}{c(x)} \cdot \delta_{ij}^x(e_\chi) = \sum_{i=1}^S \bar{\mu}_i^{xy}(e_{X_c}^w, e_{Y_c}^w) \cdot \delta_i^x(e_\chi) \quad (11)$$

Fixing ($e_{X_c}^w, e_{Y_c}^w$) in the middle of the P th zone under the assumption that the contribution from the other zones is near zero yields

$$\begin{aligned} y|_{e_{X_c}^w, e_{Y_c}^w} &= \bar{\mu}_P^{xy}(e_{X_c}^w, e_{Y_c}^w) \cdot \delta_P^x(e_\chi) + \sum_{\substack{i=1 \\ i \neq P}}^S \bar{\mu}_i^{xy}(e_{X_c}^w, e_{Y_c}^w) \cdot \delta_i^x(e_\chi) \\ &\cong \bar{\mu}_P^{xy}(e_{X_c}^w, e_{Y_c}^w) \cdot \delta_P^x(e_\chi) \end{aligned} \quad (12)$$

Equation (12) shows that, once the fuzzy sets for the position errors ($e_{X_c}^w, e_{Y_c}^w$) are fixed, the definition of fuzzy sets for e_χ should be computed by looking first at each area on the XY plane and then adding the cumulative result. Under this assumption, seven fuzzy sets were defined for the heading error e_χ : [$N_b, N_m, N_s, ZE, P_s, P_m, P_b$]. With $S = 15$ groups, each with $K = 7$ fuzzy membership functions, a total of 105 rules must be then defined. In fact, only 70 rules were defined, the fuzzy interpolation feature was exploited for the missing rules. Reference 6 contains the complete listing of all the fuzzy rules used to create the fuzzy controllers. Figure 3 shows the membership functions for e_χ and Fig. 4 shows those for $e_{X_c}^w$ and $e_{Y_c}^w$. The S fuzzy areas are shown in Figs. 4 and 5 by the level contours F of the membership functions $\mu_i^{xy}(e_{X_c}^w, e_{Y_c}^w)$; that is,

$$F(e_{X_c}^w, e_{Y_c}^w) = \max_{i=1..S} \mu_i^{xy}(e_{X_c}^w, e_{Y_c}^w) \quad (13)$$

The fuzzy sets were designed assuming a fixed aircraft velocity $V^* = 25$ m/s, whereas the scaling factor $S(V^w, V^*)$, defined in Eq. (6), makes it possible to manage different waypoint crossing speeds V^w . Figure 5 shows, as an example, the different approach trajectories to the waypoint at a velocity of 38 m/s; the figure presents a magnification of the waypoint area that highlights how the scaling factor has enlarged the fuzzy areas with respect to the nominal velocity case, thus inducing larger turn radii.

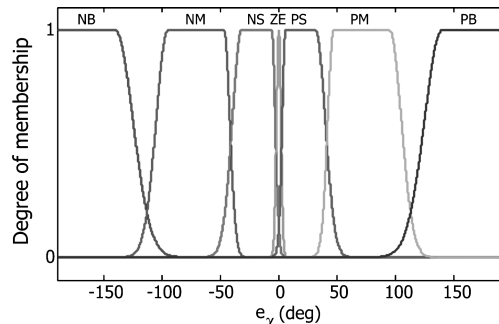


Fig. 3 Membership functions for e_χ .

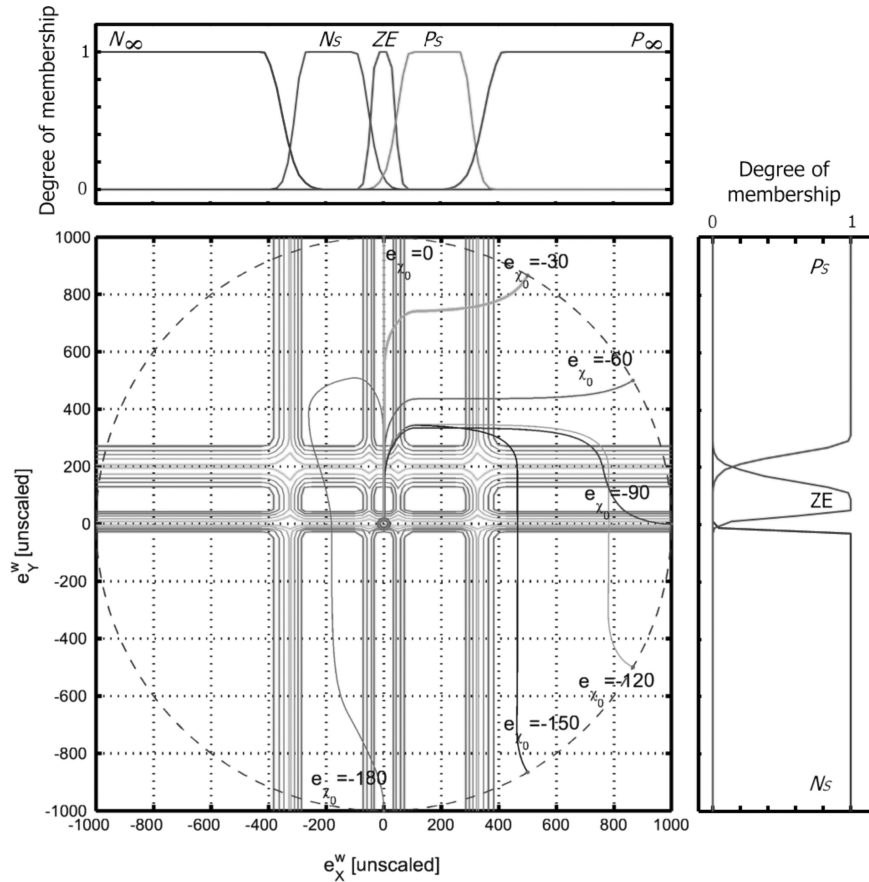


Fig. 4 Membership functions for $e_{X_c}^w$ and $e_{Y_c}^w$ and contour plots of $\mu_i^{xy}(e_{X_c}^w, e_{Y_c}^w)$.

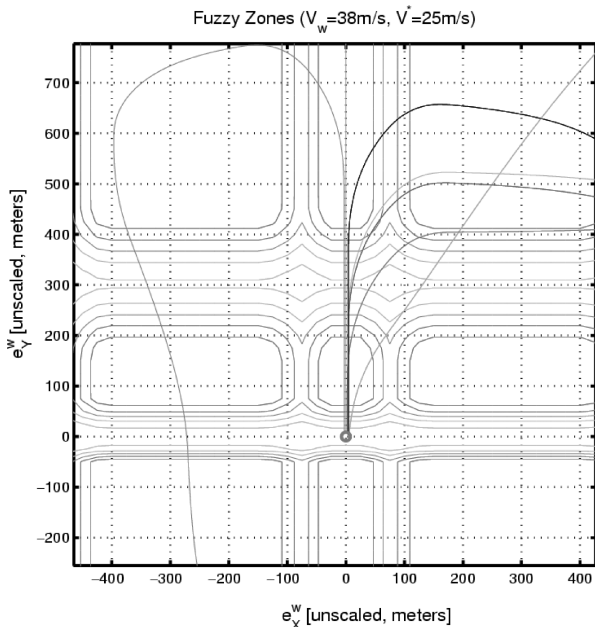


Fig. 5 Contour plots of $\mu_i^{xy}(e_{X_c}^w, e_{Y_c}^w)$ scaled membership functions.

V. Simulation Results

The fuzzy guidance system was tested first with the simple linear decoupled model and then with a fully nonlinear autopiloted aircraft model. The latter model is a jet-powered YF-22 scale aeromodel with a PC-104 onboard computer. The nonlinear mathematical model and its LQG-LTR autopilots can be found in Pollini et al.¹⁰ and Napolitano.¹¹

The first two simulations presented in this section describe two nonplanar trajectories. In the first example, the aircraft is driven to waypoint W_1 ; then to align with W_2 ; then to W_3 , that is, 150 m lower in altitude and very near to W_2 on the (X, Y) plane; and finally to W_4 at altitude 100 m with a desired approach angle rotated by $(\pi/2)$ from the previous waypoint. Figure 6 shows the resulting trajectory.

The simulation results show that the required descent from W_2 to W_3 is too steep for the dynamic characteristics of the aircraft, as defined in the design phase of the fuzzy rule-set. When the aircraft reaches the X, Y coordinates of W_3 its altitude is still high, and it turns to come back to the waypoint at the prescribed altitude. The aircraft begins a spiral descent, centered on the waypoint vertical axis, decreasing altitude with the descent rate limitation given by the FGS, until the waypoint altitude is reached; it then proceeds to the next one. In this particular case, a half turn is enough to reach the altitude of W_3 ; thus, when the desired altitude is reached, it holds it and successfully crosses the waypoint to proceed to waypoint W_4 . The maneuver was completely generated by the FGS once it recognized that W_3 could not be reached directly under the maximum acceleration design constraints.

In the second example, the guidance system produces a trajectory that is intended to take the aircraft from takeoff to landing following a sequence of 10 waypoints. The results are shown in Fig. 7. In this case, W_2 is not directly reachable from W_1 , and a rerouting is developed by the FGS.

In both the examples, the alternate flight paths necessary to reach waypoints 3 and 2, respectively, were successfully derived by the fuzzy controller and were not prescribed a priori as described in Ref. 1, for instance.

In the last simulation, the FGS was applied to the YF-22 scaled aeromodel described in.^{10,11} A reference model, based on Eq. (1), and appropriate rate limiters on the three FGS outputs were inserted between the FGS and the autopiloted aircraft to shape the desired

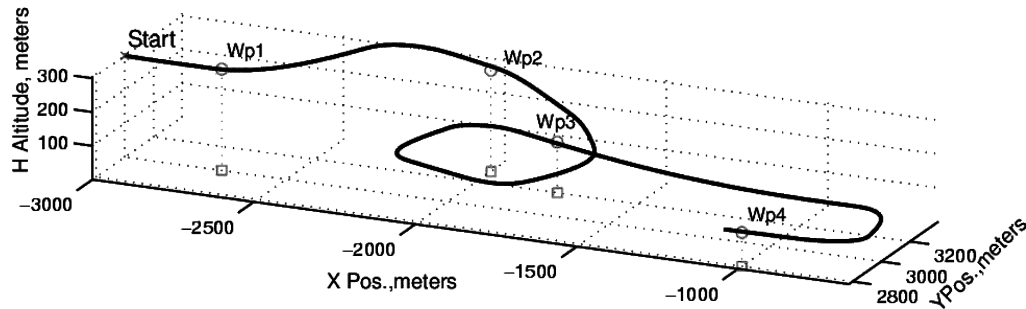


Fig. 6 Simulation of a four-waypoint trajectory.

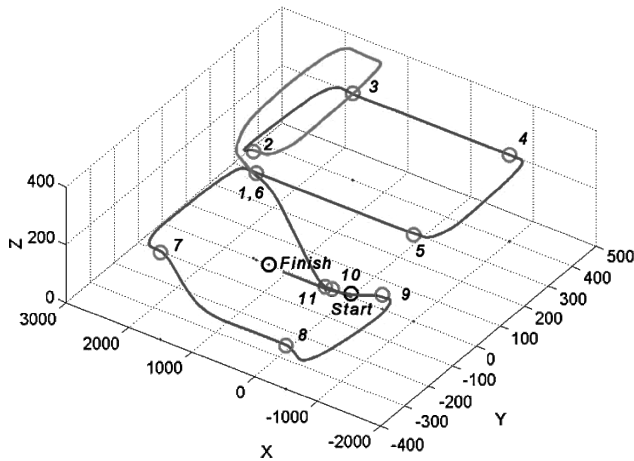


Fig. 7 Takeoff to landing trajectory (all units in meters).

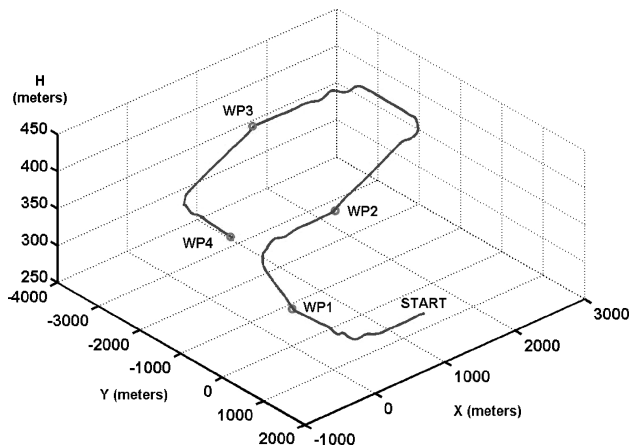


Fig. 8 YF-22 scale model simulation: trajectory.

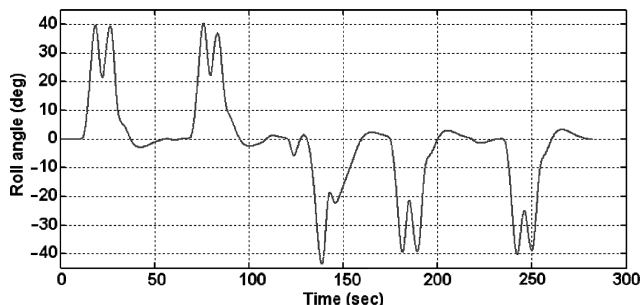


Fig. 9 YF-22 scaled model simulation: roll angle.

dynamic response. Because an altitude-hold autopilot was already present, the fuzzy altitude controller $f_y(e_H)$ was disabled, and the waypoint altitude H_W output of the WG was used directly as reference for the aircraft's own autopilot. Figure 8 shows the sample trajectory defined by four waypoints at different altitudes. The aircraft correctly crosses the four waypoints, whereas a little altitude drop is noted during turns. Figure 9 shows the roll angle of the aircraft during the flight.

VI. Conclusions

This Note presents a five-dimensional waypoint-based fuzzy guidance system (FGS) for unmanned aircraft vehicles. Computer simulations show that the aircraft correctly crosses all waypoints in the specified order. The FGS deals with unflyable waypoints as well, driving the aircraft on flyable trajectories that try to cross the waypoints at the prescribed altitude and with the prescribed heading. The guidance system, although not designed for rejection of atmospheric disturbances, was shown to be able to define flyable trajectories, even in the presence of a speed differential between the initial trim conditions and the waypoint crossing speed.

Acknowledgments

Part of the work was performed under Contract EOARD-F61775-02-WE031, with Neal Glassman as Technical Monitor. The support of European Office for Aerospace Research and Development (EOARD), Air Force Office for Scientific Research (AFOSR), and Air Force Research Lab. (AFRL)/MNA is greatly appreciated.

References

- Menon, P. K., and Iragavarapu, V. R., "Blended Homing Guidance Law Using Fuzzy Logic," AIAA Paper 98-4304, Aug. 1998.
- Lin, C.-F., *Modern Navigation Guidance and Control Processing*, Prentice-Hall, Upper Saddle River, NJ, 1999.
- Takagi, T., and Sugeno, M., "Fuzzy Identification of Systems and Its Applications to Modelling and Control," *IEEE Transactions*, Vol. 15, No. 1, 1985, pp. 116-132.
- Whang, I. H., and Hwang, T. W., "Horizontal Waypoint Guidance Design Using Optimal Control," *IEEE Transactions on Aerospace and Electronic Systems*, Vol. 38, No. 3, 2002, pp. 1116-1120.
- Pollini, L., Baralli, F., and Innocenti, M., "Waypoint-Based Fuzzy Guidance for Unmanned Aircraft—A New Approach," AIAA Paper 2002-4993, Aug. 2002.
- Turra, D., "Sistemi di Guida Fuzzy per Inseguimento di Waypoints," M.E. Thesis, Univ. of Pisa, Pisa, Italy, Oct. 2002; available at URL: <http://www.dsea.unipi.it/DSEA/Personnel/PhDStudent/DemetrioTurra/thesis.ps> [cited 25 March 2004].
- Pollini, L., Giulietti, F., and Innocenti, M., "SNIPE: Development of an Unmanned Aerial Vehicle at DSEA—University of Pisa," *Proceedings of 15th Bristol International Conference on UAV's Conference 2000*, Dept. of Aerospace Engineering, Univ. of Bristol, Bristol, England, U.K., 2000.
- Pollini, L., Giulietti, F., and Innocenti, M., "SNIPE: Development of an Unmanned Aerial Vehicle at DSEA—University of Pisa," *Proceedings of UAV 2000 Conference Paris*, 2000.
- Giulietti, F., Pollini, L., and Innocenti, M., "Waypoint-Based Fuzzy Guidance for Unmanned Aircraft," *Proceedings of the 15th IFAC Symposium on Automatic Control in Aerospace*, International Federation of Automatic Control, Laxenburg, Austria, 2001.

¹⁰Pollini, L., Mati, R., Innocenti, M., Campa, G., and Napolitano, M., "A Synthetic Environment for Simulation of Vision-Based Formation Flight," AIAA Paper 2003-5376, Aug. 2003.

¹¹Napolitano, M., West Virginia Univ., Air Force Office of Scientific Research Grant F49620-98-1-0136, Final Rept., March 2002.

Gain-Scheduling Stability Issues Using Differential Inclusion and Fuzzy Systems

Mario Innocenti,* Lorenzo Pollini,[†]
and Antonio Marullo[‡]
University of Pisa, 56126 Pisa, Italy

I. Introduction

SINCE its first appearance, the Takagi–Sugeno (TS) fuzzy model theory¹ has proven useful in the description of nonlinear dynamic systems as a means of blending of models obtained by local analysis. Such descriptions are referred to as model-based fuzzy systems (MBFS). In addition, the TS approach can be used for the synthesis of fuzzy gain-scheduled controllers. The stability of MBFS was studied by Hallendorn et al.,^{2,3} who defined a stability test by imposing some conditions on the local control laws. The present work describes a new stability criterion, which relaxes the bounds in Ref. 3, yielding a less conservative condition. Two case studies are presented comparing the use of off-equilibrium vs equilibrium grid points and fuzzy vs crisp scheduling.

II. Modeling and Control

Consider a nonlinear continuous and continuously differentiable system of the form

$$\dot{\bar{x}} = f(\bar{x}, \bar{u}), \quad \bar{y} = \bar{x} \quad (1)$$

where $\bar{x} \in \mathbb{R}^n$, $\bar{u} \in \mathbb{R}^m$, and $f : \mathbb{R}^n \times \mathbb{R}^m \rightarrow \mathbb{R}^n$. We wish to design a controller capable of following some desired trajectory (\bar{x}_r, \bar{u}_r) , where \bar{x}_r is a differentiable, slowly varying state trajectory and \bar{u}_r is the nominal input necessary to follow the unperturbed \bar{x}_r state.^{2,3} Let us define a subset $XU \subset \mathbb{R}^{n+m}$ of the system's state and input spaces as a bound on all of the possible state and input values. Let us also define a set of operating points as $(x_i, u_i) \in XU$, $i \in I$ with I set of all positive integers that form a regular (or irregular) grid J in the trajectory space. Linearization of Eq. (1) about all of the points in J yields

$$A_i = \left. \frac{\partial f}{\partial x} \right|_{(x_i, u_i)}, \quad B_i = \left. \frac{\partial f}{\partial u} \right|_{(x_i, u_i)} \quad (2)$$

resulting in perturbed dynamics about the linearization points given by

$$\dot{\bar{x}} = A_i(\bar{x} - \bar{x}_i) + B_i(\bar{u} - \bar{u}_i) + f(\bar{x}_i, \bar{u}_i) = A_i\bar{x} + B_i\bar{u} + \bar{d}_i \quad (3)$$

$$\bar{d}_i = f(\bar{x}_i, \bar{u}_i) - A_i\bar{x}_i - B_i\bar{u}_i$$

Received 27 June 2003; revision received 23 July 2003; accepted for publication 23 July 2003. Copyright © 2003 by the American Institute of Aeronautics and Astronautics, Inc. All rights reserved. Copies of this paper may be made for personal or internal use, on condition that the copier pay the \$10.00 per-copy fee to the Copyright Clearance Center, Inc., 222 Rosewood Drive, Danvers, MA 01923; include the code 0731-5090/04 \$10.00 in correspondence with the CCC.

*Full Professor, Department of Electrical Systems and Automation, Via Diotallevi 2. Associate Fellow AIAA.

[†]Postdoctoral Fellow, Department of Electrical Systems and Automation, Via Diotallevi 2.

[‡]Graduate Student, Department of Electrical Systems and Automation, Via Diotallevi 2.

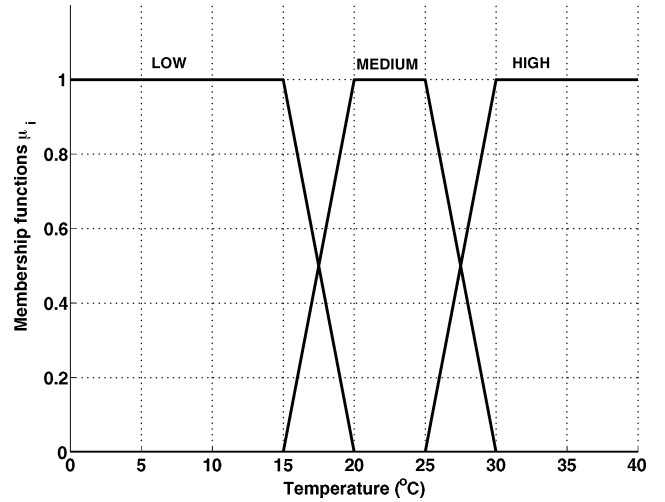


Fig. 1 Example of fuzzy rule set.

When the linearized systems (3) are interpolated through a TS model, a nonlinear approximation of Eq. (1) is obtained, given by

$$\dot{\bar{x}} \cong \hat{f}(\bar{x}, \bar{u}) = \sum_{i \in I} \mu_i(\bar{x}, \bar{u}) \cdot (A_i\bar{x} + B_i\bar{u} + \bar{d}_i) \quad (4)$$

A fuzzy control law for system (4) is also designed as a gain-scheduling controller based on a TS model. Under the hypothesis of controllability for all $(A_i, B_i) \forall i \in I$ and being all of the states measured, full-state feedback linear control laws can be synthesized and interpolated through a fuzzy TS system yielding

$$\begin{aligned} \bar{u} &= \bar{u}_r + \sum_{j \in I} v_j(\bar{x}, \bar{u}) \cdot K_j[(\bar{x} - \bar{x}_j) - (\bar{x}_r - \bar{x}_j)] \\ &= \bar{u}_r + \sum_{j \in I} v_j(\bar{x}, \bar{u}) \cdot K_j[\bar{x} - \bar{x}_r] \end{aligned} \quad (5)$$

In Eqs. (4) and (5) the expressions μ_i, v_j represent the TS linear membership functions relating the input variables to the fuzzy domain described by IF-THEN-ELSE rules consequent. The fuzzy system membership functions are chosen such as they constitute a convex sum over the input range XU . An example is shown in Fig. 1.

Substituting Eq. (5) in Eq. (4), the closed-loop perturbed system dynamics become

$$\begin{aligned} \dot{\bar{x}} - \dot{\bar{x}}_r &= \sum_i \mu_i(\bar{x}, \bar{u}) \cdot \left\{ A_i + B_i \left[\sum_j v_j(\bar{x}, \bar{u}) K_j \right] \right\} (\bar{x} - \bar{x}_r) + \varepsilon \\ \varepsilon &= \sum_i \mu_i(\bar{x}, \bar{u}) \cdot (A_i\bar{x}_r + B_i\bar{u}_r + \bar{d}_i) - \dot{\bar{x}}_r \end{aligned} \quad (6)$$

Note that the term $\sum_i A_i\bar{x}_r$ is added and subtracted so that the matrix

$$\sum_i \mu_i(\bar{x}, \bar{u}) \cdot \left\{ A_i + B_i \left[\sum_j v_j(\bar{x}, \bar{u}) K_j \right] \right\} \quad (7)$$

gives the dynamics of the perturbation from the desired trajectory. Also, from the definition of \bar{d}_i ε represents the error with respect to \bar{x}_r as a result of the approximation of f with the TS model.

III. Stability Analysis

Let us now derive the asymptotic stability conditions of the TS fuzzy gain-scheduling controller around (\bar{x}_r, \bar{u}_r) .

Definition: Given the grid point set J and any linearized dynamics (A_i, B_i) , $i \in J$, J_i is defined as the set of all indexes m of the neighbourhood points of (\bar{x}_i, \bar{u}_i) , whose controllers K_m have a non-negligible influence over (A_i, B_i) .